Generic R&D Proposal: Z-Tagging Mini DIRC

Wenliang Li*[1,2], Charles E. Hyde*†[3], Vitaly Baturin[3], Jan Bernauer[1,2], Jaydeep Datta[1,2], Klaus Dehmelt[1,2], Abhay Deshpande[1,2], Roman Dzhygadlo[5], Prakhar Garg[1,2], Ruthie Gu[1], Thomas K. Hemmick[1], Yordanka Ilieva[6], Grzegorz Kalicy[4], Brynna Moran[1], Pawel Nadel-Turonski[2], Barak Schmookler[7], Jochen Schwiening[5], Carsten Schwarz[5], and Nilanga Wickramaarachchi[4]

[1]Stony Brook University, Stony Brook, NY 11794, USA
[2]Center for Frontiers in Nuclear Science, Stony Brook University, Stony Brook, NY 11794, USA
[3]Old Dominion University, Norfolk VA 23529, USA
[4]Catholic University of America, Washington D.C. 20064, USA
[5]GSI Helmholtz Centre for Heavy Ion Research, Darmstadt, Germany
[6]University of South Carolina, Columbia South Carolina 29208, USA
[7]University of California Riverside, Riverside, CA 92521, USA

July 25, 2022

Abstract

We propose an R&D program for a fused silica Cherenkov detector at the high dispersion downstream ion focus of the Interaction Region (IR) of a proposed second detector at the 8:00 o'clock position on the EIC ring. The goal of the detector is to resolve the discrete charge of nuclear fragments produced in eA collisions. This capability would greatly enhance the ability to separate coherent nuclear processes from incoherent channels. Tagging the charge of nuclear fragments in coincidence with detection of decay photons would enable a unique program of rare isotope spectroscopy with nuclear half-lives as short as ~ 1 nsec. We will simulate the Cherenkov light production primary ions, secondary δ-rays and other background sources. We will evaluate the challenges of recording light pulses with a 10,000:1 dynamic range.

Total proposed year one budget is $\$114,000$.

*Co-spokesperson
†Contact person, chyde@odu.edu

Contents

1 Introduction & Motivation **2**

2 Cherenkov Signal **4**
2.1 Fused Silica 4
2.2 Ray Trace Simulations 5
2.3 Energetic δ-Rays 6
2.4 Gain Saturation Effects 7

3 Background Studies **8**

4 Light Collection and Photo-Sensor Studies **8**
4.1 Year One Deliverables 9
4.2 Quartz Manufacturing Quality Control 9

5 Prototype and Beam Tests **10**
5.1 Year 2 10
5.2 Year 3 10

6 Equity **10**
6.1 Cost Effectiveness 10
6.2 Diversity, Equity, and Inclusion 10
6.3 Post-Doc and Graduate Student Support and Mentoring 10

7 Year One Budget **11**

References **12**

1 Introduction & Motivation

Recent studies have illustrated the potential of the Electron Ion Collider (EIC) to detect short-lived rare isotopes produced in eA collisions [3]. The daughter isotopes are generally produced as either evaporation residues (ER) or fission fragments (FF). In either case, the daughter isotopes have a magnetic rigidity close to the original beam ion, but slightly different due to the variable charge-to-mass ratios of the daughter ions. In addition, evaporation residues are created with only minimal transverse momentum relative to the ion beam axis. Even fission fragments receive a transverse kick less than twice the RMS transverse momentum of the ion beam at the Interaction Point (IP). The potential for resolving ERs from the ion beam is illustrated in Fig. 1, both for the Project Detector Interaction Region 6 (IR6) ion optics and for proposed IR8 ion optics. The Interaction Region 8 (IR8) proposed for a second detector includes with a high dispersion second focus approximately 48 m downstream of

the interaction point (IP). The physics potential of rare isotope tagging at a second IR was highlighted in the DPAP report [1].

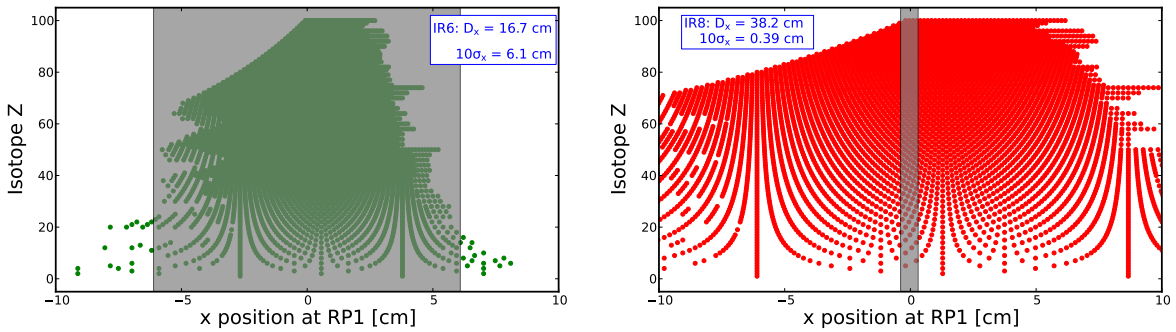

Figure 1: Isotope z vs. hit position in the best Roman pot in IR6 (left) and IR8 (right), respectively [3]. The gray box on each plot shows the 10σ beam size which prevents detection. This exclusion is much smaller in IR8 due to the 2^{nd} focus. The larger horizontal spacing in IR8 is due to a larger dispersion. The isotopes shown assume a ^{238}U beam, but are representative for all heavy ions. The exceptional ability of IR8 to detect fragments with magnetic rigidities very close to that of the beam is also indicative of the acceptance for recoil protons and nuclei that emerge from exclusive reactions with a low p_T with respect to the beam.

The Zero Degree Calorimeter (ZDC) and the gap inside of the first downstream dipole–B0 (but outside the beam pipe) can be instrumented with high resolution electromagnetic calorimetry to detect boosted decay photons in coincidence with the tagged ion at the second focus. In this way the excitation spectra of rare isotopes can be measured, particularly for short lived isotopes that are not accessible at FRIB and other facilities.

Tagging ion beam fragments is also essential for resolving coherent deep virtual exclusive scattering processes (*e.g.* $e + Pb \rightarrow e' + J/\Psi + Pb$) from incoherent scattering in which one or more nucleons are emitted.

In this proposal, we describe an R&D program for a small detector capable of identifying the nuclear charge z of ion fragments detected in the Roman Pots (RP) at the second focus. This mini Detector of Internally Reflected Cherenkov light (mini-DIRC) would consist of a thin quartz radiator coupled to a light collection volume and a high resolution photo-sensor. The z-dependent signal is the event-by-event absolute intensity of the Cherenkov light pulse.

The mini-DIRC design goal is to measure the light pulse from a heavy projectile with relative stability $\leq 1\%$ for $z = 90$.

2 Cherenkov Signal

In a medium of index of refraction $n(\lambda)$, the Cherenkov photon emission per unit length dX along the particle track and per unit wavelength for a particle of velocity $\beta > 1/n(\lambda)$ is [5]:

$$\frac{dn_\gamma(\lambda)}{dXd\lambda} = z^2 \frac{2\pi\alpha}{\lambda^2}\left[1 - \frac{1}{\beta^2 n^2(\lambda)}\right] \tag{1}$$

2.1 Fused Silica

The index of refraction of fused silica, from the near UV to near IR is plotted in Fig. 2. This is also described by the dispersion equation [4]:

$$n^2(\lambda) - 1 = \frac{0.6962}{1 - [(68.40\text{ nm})/\lambda]^2} + \frac{0.4079}{1 - [(116.2\text{ nm})/\lambda]^2} + \frac{0.8975}{1 - [(9.896\,\mu\text{m})/\lambda]^2} \tag{2}$$

Given a photo-sensor of quantum efficiency $\epsilon(\lambda)$ (which also depends on position on the sensor) and a light collection acceptance $a(\lambda)$ (which is also a transfer function from particle position to position on sensor), the projected number of detected photo-electrons is

$$N_{p.e.}(z) = \Delta X \int d\lambda \frac{dn_\gamma(\lambda)}{dXd\lambda}\epsilon(\lambda)a(\lambda) \tag{3}$$

Based on the BABAR and PANDA DIRC experience, we anticipate a detection threshold of 280 nm. Integrating over the quantum efficiency of a Hamamatsu MCP-PMT R10754-07-M16 [2] and applying a 50% collection efficiency implies a total signal of $2{\cdot}10^5$ photo-electrons for a relativistic ion of $z = 90$ incident on a 0.6 cm thick SiO_2 bar. The collection efficiency, quantum efficiency and spectral range are all subject to revision and optmization. In any case, it is clear that the raw photo-emission is more than sufficient to achieve $\delta z/z \leq 1\%$ at $z = 90$. On the other hand, a successful detector must control any event-by-event fluctuations in light collection, quantum efficiency, gain non-linearity and noise (both electronic and particle background.

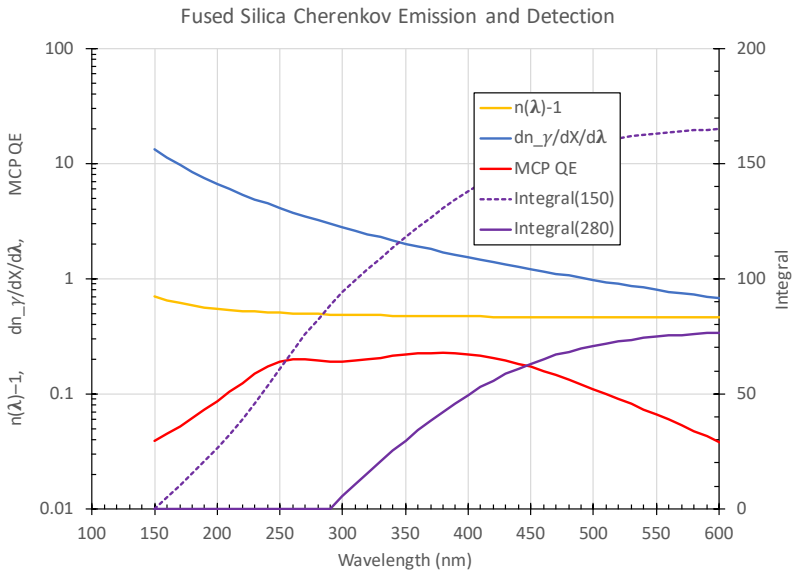

Figure 2: Index of refraction of SiO_2 (Yellow curve: $n(\lambda) - 1$) [4]. Cherenkov light yield (blue curve, projectile charge $z = 1$), units: 1/nm/cm. Quantum efficiency of Hamamatsu MCP PMT (Red curve) [2]. Integral of Eq. 3 (purple curves, right vertical axis), with charge $z = 1$, $\Delta X = 1$ cm and $a(\lambda) = 1$. Light collection and detection thresholds are $\lambda = 150$ and 280 nm for the dashed and solid curves, respectively.

2.2 Ray Trace Simulations

We have conducted an initial simulation of a $z = 90$ ion passing through a 1 cm thick SiO_2 radiator coupled to an expansion volume. This is shown in Fig. 3. Qualitatively, the photosensor surface is uniformly illuminated. The comparison of the photon yield for $z = 90$ and $z = 91$ ions in Fig. 4 shows excellent separation.

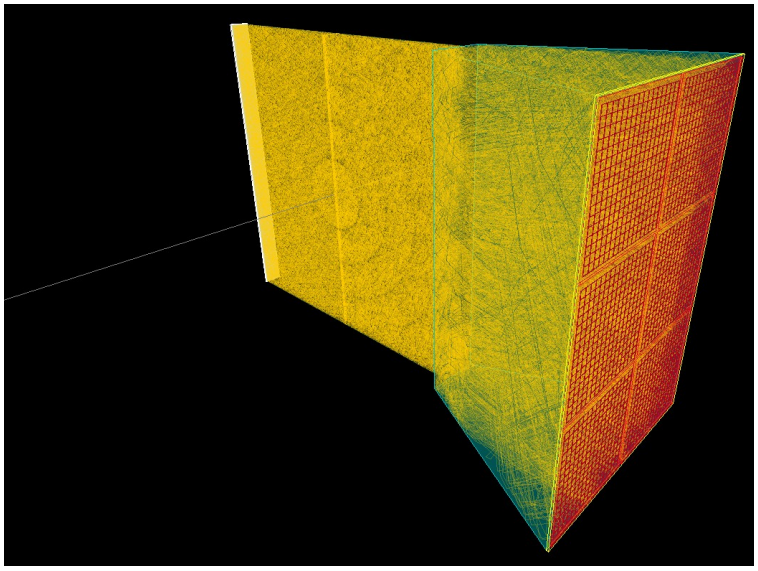

Figure 3: Ray trace of 10% of Cherenkov photons from a relativisitic $z = 90$ ion, passing through a 1 cm thick silica radiator. The light collection efficiency is 95%.

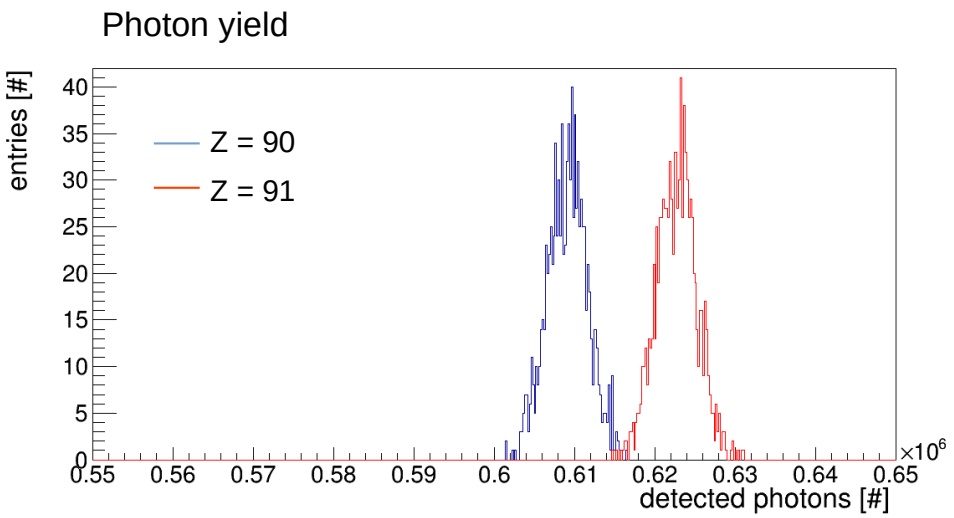

Figure 4: Comparison of the photon detection yield for $z = 90$ and $z = 91$ ions. The photo detection quantum efficiency is 30% for 280 nm to 400 nm. The statistical fluctuations correspond to only 10% of the Cherenkov yield, but the histogram is rescaled to the full yield.

2.3 Energetic δ-Rays

In addition to the direct Cherenkov light of the primary ion, there may be a significant (and fluctuating) signal from energetic secondaries (δ-rays) produced by passage of the primary ion through the quartz. The distribution of secondary electron of energy T_e, with $I \ll T_e \ll W_{\rm Max}$, is [5]:

$$\begin{aligned}
\frac{d^2N_\delta}{dX\,dT} &\approx \frac{z^2 K\rho}{2\beta^2}\left\langle\frac{z}{A}\right\rangle\frac{1}{T_e^2}\\
K &= 0.307\frac{\text{MeV cm}^2}{\text{mole}}\\
W_{\rm Max} &= \frac{2m_e\beta^2\gamma^2}{1+2\gamma m_e M_z+(m_e/M_z)^2}\\
I(\text{SiO}_2) &= 139\text{eV}, \qquad \rho(\text{SiO}_2) = 2.20\ \text{g/cm}^3.
\end{aligned} \tag{4}$$

Note that δ-ray production also scales as the projectile charge squared (z^2). The δ-ray threshold for visible Cherenkov radiation in fused silica is $T_e = T_{\rm Th} = 210$ KeV. The integrated flux of secondary electrons above Cherenkov threshold in SiO_2 is

$$\frac{dN}{dX} \approx z^2\,(0.013/\text{cm}) = \frac{106}{\text{cm}} \text{ for } z = 90. \tag{5}$$

With the same light collection assumptions described above, each of these secondaries with produce on average approximately 38 Cherenkov photo-electrons (Fig. 2), for a total yield

from an ion $z = 90$ of 4000 photo-electrons, which is just over 1% of the direct Cherenkov yield.

2.4 Gain Saturation Effects

We give here a semi-analytic estimate of gain saturation effects if SiPMs are chosen as the photo sensor. More detailed numerical simulations will be carried out if this project is funded.

Based on the previous analysis we assume $N_{pe} = 2.4 \cdot 10^5$ photo-electrons are produced by a $z = 90$ ion in a 30×30 mm^2 SiPM array. With 3×3 mm^2 readout pixels, each pixel contains 90,000 micropixels ($(10\,\mu\text{m})^2$ each) and the total number of micropixels in the full array is $N_{\mu P} = 9 \cdot 10^6$. The average occupancy per micropixel is then $\mu = N_{pe}/N_{\mu P} = 2.7\%$. Given a single photon pulse amplitude of S_0, The total signal is

$$S = N_{\mu P} S_0 \left(1 - e^{-\mu}\right) = N_{pe} S_0 \left(1 - e^{-\mu}\right)/\mu \qquad \Rightarrow 0.987 N_{pe} S_0 \quad \text{at } \mu = 2.7\% \tag{6}$$

With $N_{pe} = z^2 n_0$, the z-dependent gain saturation effect is

$$S(z) = z^2 n_0 S_0 \left(1 - e^{-\mu}\right)/\mu = N_{\mu P} S_0 \left(1 - e^{-z^2 n_0 / N_{\mu P}}\right) \tag{7}$$

To resolve ions $z \pm 1$, we require

$$\begin{aligned} \frac{1}{z} < \frac{1}{S(z)} \frac{dS}{dz} &= \frac{2\mu e^{-\mu}}{z\left(1 - e^{-\mu}\right)} \\ \left(1 + 2\mu\right) e^{-\mu} > 1 \qquad &\Rightarrow \quad \mu < 1.25 \end{aligned} \tag{8}$$

Thus the individual micro-pixel saturation does not seem to be a problem, even if larger (*e.g.* $(25\,\mu\text{m})^2$ micro pixels are used).

A second gain saturation question is whether the large amplitude pulses with reduce the gain by drawing too much charge from the bias capacitance. For the Hamamatsu S14160-3110PS MPPS, a single $(3\text{ mm})^2$ readout pixel has a capacitance of 530 pF. At a gain of $G = 2 \cdot 10^5$, a $z = 90$ ion will produce a single channel pulse

$$\begin{aligned} S_{\text{Channel}} &= (2.4 \cdot 10^3 \text{p.e.})(2 \cdot 10^5 e) \\ &= 77 \text{ pC} \end{aligned} \tag{9}$$

The gain varies as $dG/dV \approx 0.4 \cdot 10^5$ per Volt. This implies a gain shift of 0.3% between a $z = 90$ and $z = 89$ ion, whereas the signal difference is 2.2%.

In conclusion, a variety of semi-analytic tests support the idea that a thin quartz radiator can resolve the charge of incident ions with a resolution $\sigma(z) < 1$ across the chart of nuclides. We believe this concept warrants more comprehensive numerical simulation and possible prototype tests.

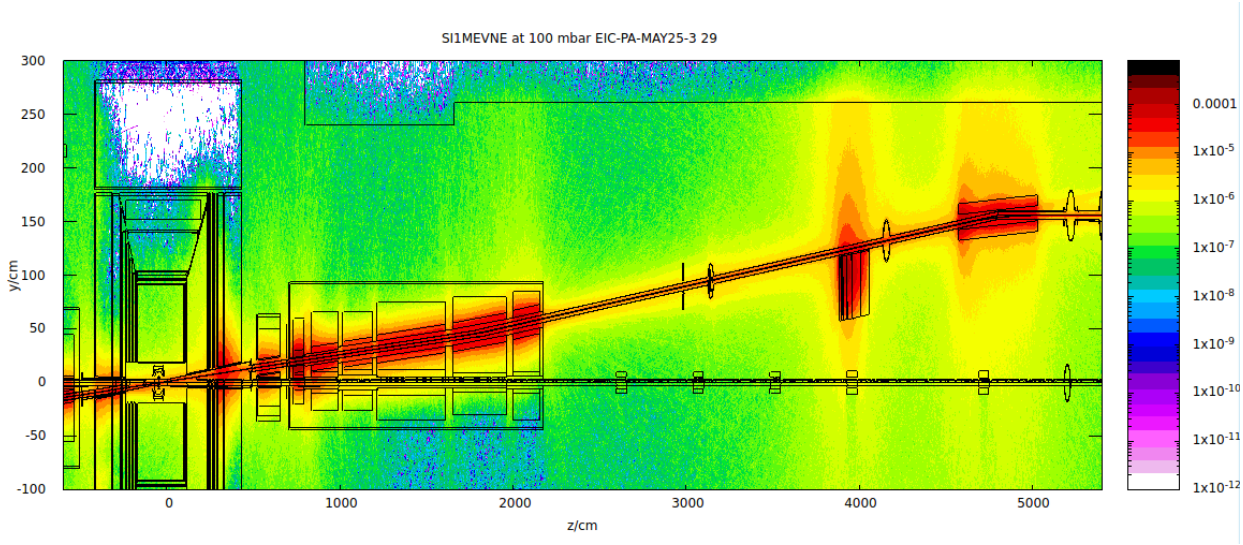

Figure 5: Neutron 1 MeV equivalent fluence in the ion downstream area (IP at -50 cm). Neutron fluence (color scale, neutrons/cm^2) is given per primary proton and at residual gas pressure $P_F = 100$ mbar. Horizontal scale: z coordinate opposite electron beam axis in cm. Vertical scale: horizontal coordinate (Y) in cm. The proton beam may be seen in this plot as a black line ("snake") following the two bending magnets. ZDC is at 40 m. Actual neutron fluence with 1 A protons and 10^{-9} mbar is obtained by multiplying color scale by $6.25 \cdot 10^7$/sec. With this scaling, maximal fluence in the ZDC is $2 \cdot 10^4$n/cm^2/s.

3 Background Studies

In eRD21, we performed FLUKA simulations of backgrounds in the EIC detector from proton beam – residual gas interactions, and the physics *ep* collisions. Fig.5 illustrates the beam-gas generated backgrounds for IR6 (Project Detector). The FLUKA model includes all beam line elements within ± 50 m of the IP. For this project, we will adapt the model for IR8. This includes increasing the crossing angle at the IP from 25 to 35 mrad and switching the polarity of the first downstream ion dipole (B0). This moves the ZDC to the outside of the ion beam. Instead of the dipole at ~ 48 m, a dipole/quadrupole pair are introduced at 35-40 m. The full ion optics produces a high dispersion focus 48 m downstream of the IP. The primary purpose of new background studies will be to understand the backgrounds in the Roman Pot detectors that would surround this second focus.

4 Light Collection and Photo-Sensor Studies

We will use the GSI DIRC simulation code to evaluate various performance issues of the proposed detector. The starting geometry is as follows:

- A fused silica bar, 0.6 cm thick along the beam direction, 3 cm tall, and 30 cm wide perpendicular to the beam direction.

- An expansion volume 3 cm long, spreading the light out to a $3 \times 3\text{cm}^2$ photo-sensor surface.
- Various potential photo-sensors, including SiPMT/MPPC, MCP-PMT, and conventional PMT.

4.1 Year One Deliverables

The raw Poisson photo-statistics are more than sufficient to resolve *e.g.* $z = 90$ from $z = 90 \pm 1$ as well as protons from helium, and every element in between. However, there many effects and sources of background that could degrade the performance relative to pure Poisson statistics. The following potential effects will be the the focus of simulation studies in the first year

1. Variations in light collection for different impact points of the incident ion (Fig. 1).
2. Variation and uniformity of light illumination of the photo-sensor surface. This can impact gain saturation effects, particularly for SiPM or MCP-PMT photosensors.
3. Fluctuations in light yield from energetic δ-rays. These can be generated either inside the silica bar itself, or in upstream elements such as the Roman Pot window.
4. Photo sensor dynamic range and gain saturation simulation studies.
5. Backgrounds from Beam Gas interactions and rescattered particles from *ep* physics collisions at the IP. The background studies will have three parts:
   (a) Neutron fluence at the location of the photo-sensors. This will determine if SiPMs are a viable option.
   (b) Charged particle tracks in SiO_2 radiator, to determine signal backgrounds.
   (c) *eA* physics events, either from FLUKA or BEAGLE.

4.2 Quartz Manufacturing Quality Control

The generation and detection of Cherenkov photons is a key aspect of the success of the proposed detector. The optimized detector performance is based on the assumption of quartz material with quality that is equivalent to the BaBar DIRC. However, a few recent R&D efforts demonstrated that sourcing high-quality quartz material can be a challenge.

SBU holds 5 bars of 15 cm x 1 cm x 0.5 cm quartz fingers (from past R&D effort) with high manufacturing quality similar to the BaBar DIRC quartz. These will be part of the in-kind contribution from SBU to the Mini-DIRC project, and could potentially be used in a prototype. Furthermore, SBU will continue pursuing the new source of vendors for high-quality quartz and perform tests to verify the claimed specifications.

5 Prototype and Beam Tests

5.1 Year 2

Depending upon the simulation studies described above, we will request funding in year 2 as follows.

- Procurement of one or more sample photosensors for tests of dynamic range, gain saturation, and noise with a variable light source.
- Procurement of a fused silica radiator bar, light guide, and enclosure to construct a prototype for beam tests.

5.2 Year 3

Beam tests. Potential options include electrons in the test facility of the Jefferson Lab Hall D Pair Spectrometer, FermiLab proton and hadron beams, CERN test beams.

6 Equity

6.1 Cost Effectiveness

This proposal includes extensive "in-kind" contributions of expertise. We have negotiated a low off-campus indirect cost rate from the Old Dominion University Research Foundation of 26% of direct costs (excluding tuition).

6.2 Diversity, Equity, and Inclusion

All of the signatories are committed to providing a work environment that supports all participants and actively recruit members of underrepresented groups. In the experimental nuclear physics group at Old Dominion University, four of eight graduate students are women. Recent graduates from the group include Torri Jesske, currently a Post-Doc at JLab and Holly Szumila-Vance, currently a Staff Scientist at JLab.

6.3 Post-Doc and Graduate Student Support and Mentoring

The ODU Experimental Research Group will provide funding, as necessary, to sustain the Post Doc and Graduate Student at 100% FTE. This will entail proportional effort on other projects. The direct supervisor of both will be Prof. C. Hyde (ODU). The travel budget is modest, but will ensure the Post Doc and Graduate student receive mentoring and that reflects the expertise of the full collaboration.

7 Year One Budget

Project period 1 Oct 2022 – 30 Sep 2023. Budget detail for full funding of year one is listed in Table 7. Summary of budgets at 100%, 80%, or 60% are listed in Table 2.

1. Full Funding: 100%. Total budget $\$114,000$.

   - 50% FTE Post Doc (ODU)
   - 100% FTE Graduate Student (ODU)
   - Foreign travel: one visit either from ODU to GSI, or GSI to ODU/JLab for training/collaborating on GSI DIRC simulation software.
   - Domestic travel: Graduate student or Post Doc travel from ODU to SBU for consultations on photo-sensor properties and dynamic range effects.

2. 80% Funding.Total budget $\$90,000$.

   - 50% FTE Post Doc (ODU)
   - 50% FTE Graduate Student (ODU)
   - Adjusted travel

   Deliverable (section 4.1)# 4: Photo sensor saturation simulation studies will be limited in scope. Deliverable (section 4.1)# 5: Background simulations will not include eA processes.

3. 60% Funding. Total budget: $\$65,000$

   - 50% FTE Post Doc (ODU)
   - Adjusted Travel. SBU.

   Background studies will only include neutron fluence. Photo sensor simulation studies will be limited in scope.

Institutional Responsibilities (Year 1)

GSI: Provide DIRC simulation code and usage training and guidance.

ODU: Cherenkov light collection simulations. Photo sensor response simulations

SBU: Advice and guidance on challenges and solutions of photo-sensor response to pulses with event-by-event dynamic range up to 10,000:1 ($z = 90 : 1$). Quantify the requirement for manufacturing the quartz bars.

Table 1: Budget Detail: ODU (Full Funding)

Item	Description	Salary	Fringe	Subtotal
1	PostDoc (50% FTE)	$30,450	$16,005	$46,455
2	Graduate Student (100% FTE)	$29,053	$ 2,210	$31,263
3	Foreign Travel			$ 3,600
4	Domestic Travel			$ 1,789
5	Subtotal (Items 1–4)			$83,107
6	IDC: 26% of Item 4 (Off-Campus rate)			$21,608
7	Tuition (IDC exempt)			$ 9,286
8	**Total** (Items 5,6,7)			**$114,000**

Table 2: Budget Summaries (ODU)

Budget: 100%			
Item	Description	Subtotal Direct	Total with IDC
1	ODU Post Doc (50% FTE)	$46,455	$58,533
2	ODU Grad Student (100% FTE)	$40,548	$48,677
3	Travel	$5,389	$6,790
	Total 100% Budget		**$114,000**
Budget: 80%			
1	ODU Post Doc (50% FTE)	$46,455	$58,533
2	ODU Grad Student (50% FTE)	$20,855	$24,920
3	Travel	$5,196	$6,547
	Total 80% Budget		**$90,000**
Budget: 60%			
1	ODU Post Doc (50% FTE)	$46,455	$58,533
2	Travel	$5,132	$6,467
	Total 60% Budget		**$65,000**

References

[1] EIC Detector Proposal Advisory Panel report . https://www.bnl.gov/dpapanelmeeting/files/pdf/dpap_report_3-21-2022_final.pdf, 2022.

[2] Hamamatsu MCP-PMT R10754-07-M16 . URL https://www.hamamatsu.com/us/en/product/optical-sensors/pmt/pmt_tube-alone/mcp-pmt.html. Accessed on 2022-07-08.

[3] B. Moran, B. Schmookler, et al. Study of exotic nuclei made easy – a potentially novel topic for physics at the EIC, 2022. URL

https://indico.cern.ch/event/1072533/contributions/4779245/. Contribution to DIS2022.

[4] M. N. Polyanskiy. Refractive index database. https://refractiveindex.info. Accessed on 2022-07-06.

[5] R. Workman et al. Review of Particle Physics. URL https://pdg.lbl.gov. to be published in Prog. Theor. Exp. Phys. 2022, 083C01 (2022).